ELSEVIER

Journal of Alloys and Compounds 323–324 (2001) 331–335

Journal of ALLOYS AND COMPOUNDS

www.elsevier.com/locate/jallcom

EXAFS determination of the Nd^{3+} lattice position in Nd:$LiNbO_3$: influence of lithium niobate stoichiometry and Mg^{2+} and Zn^{2+} co-doping

M. Vila*, A. de Bernabé, C. Prieto

Instituto de Ciencia de Materiales de Madrid, Consejo Superior de Investigaciones Científicas, Cantoblanco, 28049 Madrid, Spain

Abstract

A set of Nd–Mg and Nd–Zn co-doped $LiNbO_3$ samples has been investigated by extended X-ray absorption fine structure (EXAFS) spectroscopy. We investigated the lattice position of the Nd^{3+} ion site to understand the effect of this location on the optical properties of co-doped $LiNbO_3$. We determined its lattice position by analyzing the local order around neodymium ions. For Mg^{2+} and Zn^{2+} concentrations higher than the characteristic Li deficiency in congruent $LiNbO_3$ crystals, the Nd^{3+} host position is near the Li-octahedron. Surprisingly, for Mg^{2+} concentrations smaller than the congruent Li deficiency, Nd^{3+} occupies a vacancy position, associated with an empty structural octahedron between the Li- and Nb- lattice sites.

Keywords: Ferroelectrics; EXAFS; Optical properties; Synchrotron radiation; X-ray and X-ray spectroscopies

1. Introduction

$LiNbO_3$ is a widely studied optoelectronic material because of its technological applications. Doping with foreign ions modifies the optical properties of the matrix and makes the system useful for a wide variety of applications, such as photorefractive devices [1], solid state lasers [2] or optical waveguides [3].

In the last few years, several studies devoted to determining the impurity lattice position using different techniques have been reported. For example, electron nuclear double resonance (ENDOR), to study the Fe^{3+} impurity position in $LiTaO_3$ congruent crystal; [4] Rutherford backscattering (RBS) based spectroscopies to determine the lattice position of Hf and Fe ions in congruent $LiNbO_3$ [5,6]. Using laser spectroscopy, the ion position distribution of Nd has been reported to be in three non-equivalent centers [7]. The lattice position of diffused Er ions into congruent $LiNbO_3$ has been determined, by the X-ray standing waves technique, to be at the Li site and displaced -0.46 Å along the *c*-axis [8]. Finally, extended X-ray absorption fine structure (EXAFS) has been used to study several ions, such as Ti, Fe, Hf and rare earths (Er, Nd) in $LiNbO_3$ crystal [9–13]. Similar conclusions have been reported in all of these works: for single doped $LiNbO_3$, the foreign ions are located near the Li sites, except for the Ta impurity [11], which substitutes Nb, as expected from the isomorphism between $LiTaO_3$ and $LiNbO_3$. The fact that congruent samples have a 4.8% Li deficiency has been claimed as the main reason for associating all of the impurities with its Li lattice site [9].

Because of the importance of the Nd^{3+} ion in solid state laser technology, its location in the $LiNbO_3$ matrix has received special attention and has been extensively studied by optical and RBS/channeling techniques [14–18]. Moreover, there is some relationship between changes in the optical properties (such as optical damage reduction) and the Mg concentration when Nd and Mg (or Nd and Zn) are present in the crystal [19]. Such optical changes have been observed for Mg concentrations larger than 5% [20]. This behavior is explained by the similar ionic radii of Mg^{2+} and Li^{+} ions. Mg fills the 4.8% Li-deficient corresponding sites in the congruent $LiNbO_3$ crystal and the reminding Mg ions cannot enter the crystal at this position. EXAFS spectroscopy provides direct information on the nature, number and bond distances of the neighboring atoms with respect to the atom tested and has proved to be a reliable tool that is complementary to the channeling techniques. From these techniques, we can obtain useful information about the lattice site location and bond distances to nearest neighbors and, therefore, displacements from the Li or Nb lattice site can be calculated.

The $LiNbO_3$ structure has been determined by neutron and X-ray diffraction [21]. The structure is made up of

*Corresponding author.

0925-8388/01/$ – see front matter
PII: S0925-8388(01)01032-5

irregular octahedra piled along the ferroelectric *c*-axis and sharing faces. The octahedra are occupied by cations in the sequence Li, Nb and a vacancy octahedron. Furthermore, both Li and Nb are displaced (in opposite senses) along the *c*-axis towards the neighboring vacancies.

2. Experimental

Congruent samples of co-doped $LiNbO_3$ single crystals were grown from melts with molar concentrations of 1% Nd_2O_3 and 6% MgO, 3% MgO and 8% ZnO, respectively.

X-ray absorption experiments were carried out at the CRG/IF beamline BM32 bending magnet, using double multilayer mirrors for harmonic suppression and vertical collimation and double-crystal Si(111) monochromator with sagittal focusing, at the European Synchrotron Radiation Facility (ESRF) in Grenoble. Nd L_{III}-edge spectra were recorded at room temperature in fluorescence detection mode using a five-element Ge detector with a total counting rate of 350 000 ph/s. For each sample, three–four scans were collected at slightly different incidence angles, in order to identify and avoid any small bragg peaks that might have been appearing.

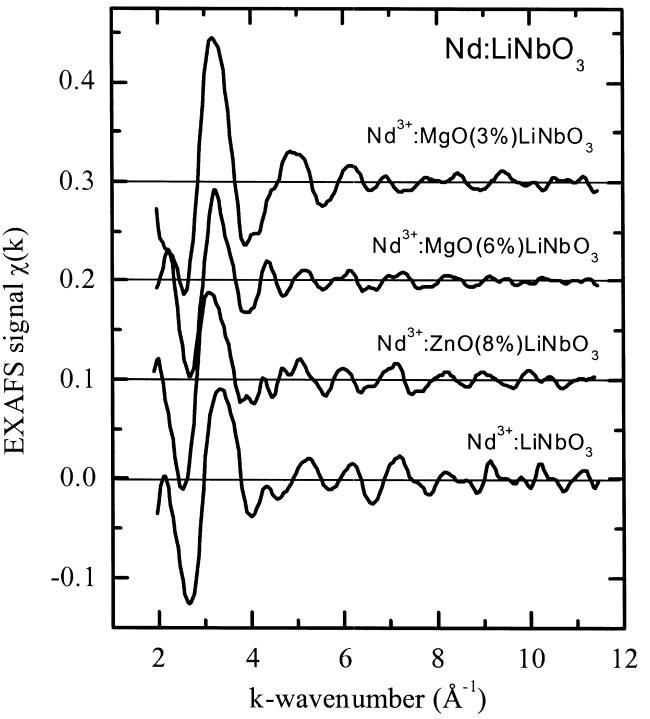

Fig. 1. EXAFS $\chi(k)$ signal obtained at the Nd L_{III}-edge in several $LiNbO_3$ single crystals: Nd^{3+}-doped $LiNbO_3$ congruent sample and Nd^{3+} co-doped $LiNbO_3$ with 8% ZnO, 6% MgO and 3% MgO.

3. Results and discussion

Fig. 1 shows the fluorescence detected EXAFS signal of Nd L_{III}-edge (6208 eV) in several $LiNbO_3$ samples. Due to the excellent beam quality from the ESRF storage ring, there is a very good signal even for an estimated 0.1% Nd concentration.

Fig. 2 shows the Fourier transform (FT) magnitude of the *k*-weighted EXAFS signals [$k\chi(k)$]. In order to allow comparison between those samples, the selected *k*-range of the $k\chi(k)$ function to perform the FT was kept constant from 1.90 to 11.50 $Å^{-1}$. This short *k*-range is imposed by the proximity of the Nd L_{II}-edge at 6722 eV, but it is sufficient to observe the second coordination sphere, which is important in locating the foreign ion in the lattice. The FT is related to the radial distribution function around the Nd^{3+} ions. As in other EXAFS studies of the position of foreign ions in $LiNbO_3$ [11], Li^+ ions give no EXAFS signal as backscatter due to their low atomic number. Moreover, due to the large decrease in their backscattering amplitude function, oxygen atoms are only observable when they are at the first coordination sphere. For example, in the congruent sample, the main two FT peaks are explained as follow: the first significant peak, at around 1.8 Å, is related to the mean distance from Nd^{3+} to the next nearest oxygen forming the characteristic octahedra; and the peak at around 3.2 Å is related to the Nd–Nb distances that form the second coordination sphere. Impurity aggregation has not been considered because a 0.1% Nd atomic

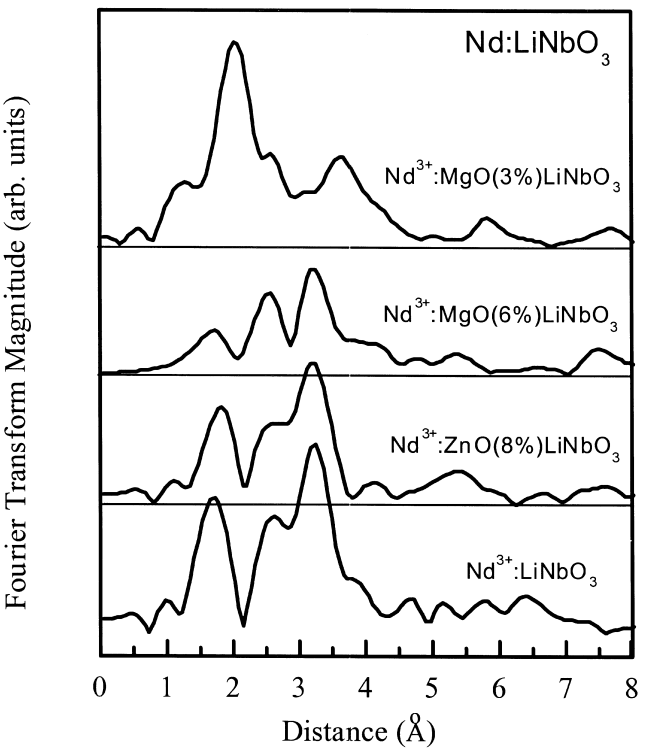

Fig. 2. Fourier transform magnitude of the $k\chi(k)$ function, showing the pseudo-radial distribution function around the Nd^{3+} ion in the studied samples of Fig. 1.

concentration seems to be too small to have this effect and because there is no experimental evidence of any aggregation.

The analysis of Fig. 2 shows that (i) the FT magnitude for 6% MgO and 8% ZnO is very similar to that obtained for Nd in the congruent $LiNbO_3$. This fact indicates that a near Li-site position is allowed for Nd^{3+} ions. (ii) Both the shape and position of the first main peak are different for the 3% MgO sample.

Before quantitative data-fitting, we introduce a picture in order to show the variation of the neighbour distances from an impurity placed along the *c*-axis of $LiNbO_3$. Fig. 3 shows the calculated distances (from $LiNbO_3$ structural data) to the oxygen and niobium atoms as a function of the displacement (δ) along the *c*-axis. The δ-displacement is defined as the distance from the Nb-site (or Li-site) moving along the (*c*-axis) line passing through the center of the triangles forming the distorted oxygen octahedra in the $LiNbO_3$ structure. In this figure, the origin of the δ-coordinate is the Nb site and δ runs over a complete lattice cell. Thus, the arrows of Fig. 3 indicate the δ values associated with the Li, Nb and the so-called vacancy position.

Table 1 shows the obtained EXAFS parameters. In order to perform the fits, the backscattering functions were calculated by using the FEFF code, version 6.01, reported by Rehr [22]. It has been assumed that there are six oxygen neighbors in an octahedral symmetry and eight niobium neighbors in a similar environment as from the Li-site position in the $LiNbO_3$ structure. During the fitting analysis of Nd-doped $LiNbO_3$ congruent sample, the distance and the Debye–Waller factor of the contributing atom shells were floated while the coordination numbers were fixed at their Li-site crystallographic values. The possibility of there being more than one different Nd–O distance to take into account any distortion of the coordination sphere was considered. A typical picture of the fits is shown in Fig. 4.

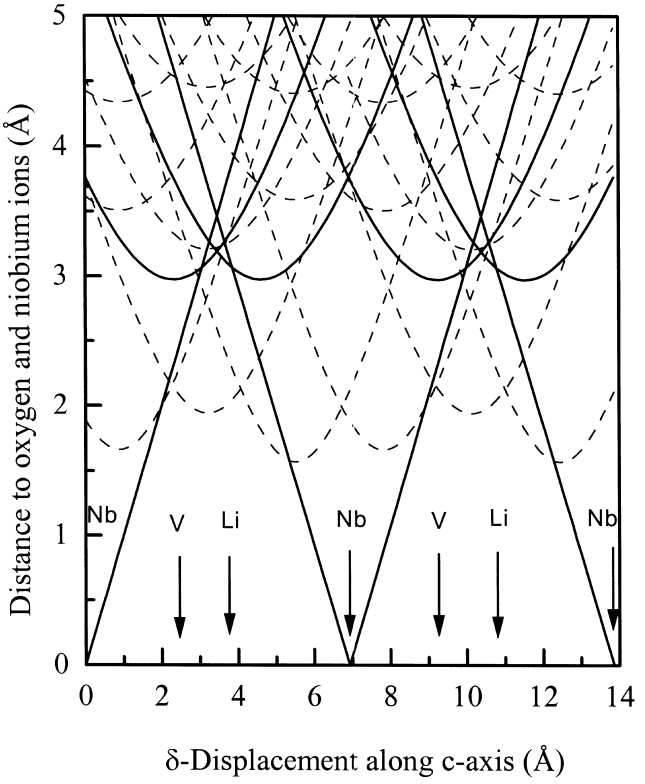

Fig. 3. Distances to the oxygen (dotted lines, Nd–O) and niobium (continuous lines, Nd–Nb) atoms as a function of the δ-displacement along the *c*-axis in $LiNbO_3$.

Table 1
EXAFS parameters obtained after fitting[a]

Sample	Pair	N_j	R_j (Å)	σ^2 (Å^2)
Nd:$LiNbO_3$	Nd–O	3.0	2.165	0.0064
(congruent)	Nd–O	3.0	3.005	0.0036
	Nd–Nb	8.0	3.35	0.0064
Nd:Zn (8%):$LiNbO_3$	Nd–O	2.0	2.262	0.0016
	Nd–O	2.7	3.000	0.0014
	Nd–Nb	7.5	3.404	0.0060
Nd:Mg (6%):$LiNbO_3$	Nd–O	1.7	2.192	0.0077
	Nd–O	0.6	2.426	0.0077
	Nd–O	3.0	3.150	0.0025
	Nd–Nb	8.0	3.350	0.0098
Nd:Mg (3%):$LiNbO_3$	Nd–O	8.5	2.390	0.0110
	Nd–Nb	3.0	2.721	0.0098
	Nd–Nb	3.0	2.920	0.0025
	Nd–Nb	4.0	3.950	0.0016

[a] N_j is the numbers of pair neighbors, R_j the pair distance and σ^2 the Debye–Waller factor.

By translating the Nd–O and Nd–Nb distances obtained from Table 1 to Fig. 3, it is possible to evaluate the position of the Nd^{3+} ions along the *c*-axis. We present these results starting by the congruent sample because it corresponds to the less distorted host lattice. Additionally, results for that sample are compared with those obtained by other techniques.

3.1. Nd in $LiNbO_3$ congruent sample

Regarding Fig. 3, it can be seen that, by moving Nd^{3+} by about 0.4 Å from the Li lattice site towards the vacancy site octahedron ($\delta = 3.35$ Å), the two Nd–O distances given in Table 1 match the oxygen branches as well as the Nd–Nb distances. The obtained shift from the *c*-axis to the eight Nb neighbors is very similar to that obtained from EXAFS. This result agrees with findings on the displacement of this foreign ion [18] obtained using the RBS/channeling technique and with a similar shift obtained for Er^{3+} (0.46 Å) by X-ray standing waves [8]. The Nd–O distances can be explained as a local rearrangement of the oxygen octahedra in a manner such that the triangle between the Li-site and the vacancy-site widens to locate the Nd^{3+} ion near the center, with a Nd–O distance of

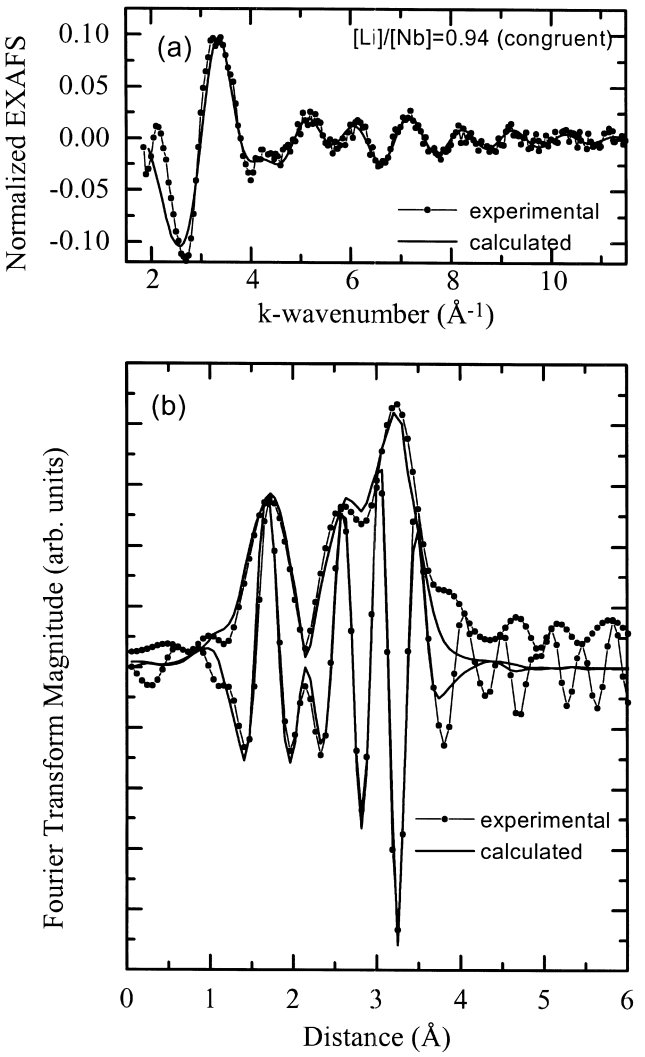

Fig. 4. (a) *k*-space comparison between the experimental and calculated $\chi(k)$ EXAFS signal for the congruent sample using the parameters given in Table 1. (b) Fourier transform of the (a)-plotted signals. Module and imaginary part have been plotted for dual comparison.

2.165 Å, and allowing the distances to the other triangles to be very similar. They appear in the fit as a single distance of about 3.0 Å. In order to explain this short-range order distortion, it must be noted that the sum of Nd^{3+} and O^{2-} ionic radii is about 2.48 Å. This corresponds to a mean Nd–O distance for the neodymium oxides whose usual coordination number is six. The present EXAFS result can be explained as follows: the Li-, Nb- and vacancy octahedra in the $LiNbO_3$ structure allow distances from their center to the six oxygens of about 2.1 Å, which is clearly too small to lodge a Nd^{3+} ion; the system reacts in such a way that it reduces the number of nearest neighbors, and the remaining nearest oxygens are moved away as much as possible. Taking into account that there are nine oxygen atoms in the neighborhood (as can be seen in Fig. 3), the lattice position that minimizes the number of nearest neighbors is the center of the triangle between the Li and the vacancy octahedra, which is displaced by 0.6 Å from the Li-site. The actual Nd position seems to be a competition between the Nd–O repulsion and the rigidity of the Nb–O bonds. EXAFS data analysis gives this position at about −0.4 Å from the Li-lattice site.

3.2. Nd in a ZnO (8%) $LiNbO_3$ co-doped sample

The TF magnitude is very similar to that obtained for the congruent single crystal. The fit indicates a small increase for the first oxygen distance (to 2.26 Å) and a reduction of the coordination number, giving a total number of approximately five oxygens for the surrounding octahedra. A similar shift of −0.4 Å from the Li-site is found for Nd ion in this sample.

3.3. Nd in a MgO (6%) $LiNbO_3$ co-doped sample

The main characteristic of this compound with respect to the ZnO co-doped sample is related to the first oxygen distance that can be resolved into two different distances (2.19 and 2.43 Å, respectively). As in the ZnO co-doped sample, the Nd–Nb distances (3.35 Å) obtained and their coordination number provide a Nd^{3+} site at the Li octahedra shifted −0.4 Å from the Li-site towards the vacancy octahedron.

3.4. Nd in a MgO (3%) $LiNbO_3$ co-doped sample

The EXAFS spectra obtained for this sample are completely different to those obtained with the preceding samples. There is a main peak centered near 2 Å, which is related to Nd–O and Nd–Nb distances. After the fitting, one can identify an oxygen sphere at 2.39 Å and a Nb sphere near 2.8 Å. In addition, there is another Nb sphere near 4 Å. With these two distances, it is clear that Nd^{3+} is placed at the vacancy octahedron site.

4. Conclusions

In order to study the influence of the lattice position on the optical properties of the Nd^{3+} ions, the local structure around neodymium in $LiNbO_3$ single crystals was determined by EXAFS. For Mg^{2+}- and Zn^{2+} concentrations higher than the characteristic Li deficiency in congruent $LiNbO_3$ crystals, the Nd^{3+} host position is near the Li-octahedron. For Mg^{2+} concentrations smaller than the characteristic Li deficiency in congruent $LiNbO_3$ crystals, the Nd^{3+} host position corresponds to a vacancy position, associated with the empty octahedron between the Li- and the Nb lattice octahedron.

Acknowledgements

This work has been partially supported by CICyT under grant number MAT97-0725. The author wishes to acknowledge Prof. J.A. García-Solé for providing samples and for very fruitful discussions on this topic. Thanks are also given for the experimental facilities provided by ESRF (ESRF project NΦ HC-598).

References

[1] E. Kratzig, O.F. Schirmer, in: Photorefractive Materials and their Applications I, Springer Topics in Applied Physics 61, Springer, Berlin, 1988.
[2] L.F. Johnson, A.A. Ballman, J. Appl. Phys. 40 (1969) 297.
[3] M.N. Armenise, C. Canali, M. de Sario, E. Zanoni, Mater. Chem. Phys. 9 (1983) 267.
[4] H. Söthe, L.G. Rowan, J.M. Spaeth, J. Phys. Condens. Matter. 1 (1989) 3591.
[5] L. Rebouta, J.C. Soares, M.F. Da Silva, J.A. Sanz-García, F. Agulló-López, J. Mater. Res. 7 (1992) 130.
[6] L. Rebouta, M.F. Da Silva, J.C. Soares, M. Hage-Ali, J.P. Stoquert, P. Siffert, J.A. Sanz-García, E. Dieguez, F. Agulló-López, Europhys. Lett. 14 (1991) 557.
[7] G. Lifante et al., Chem. Phys. Lett. 176 (1991) 482.
[8] Th. Gog, M. Griebenow, G. Materlik, Phys. Lett. A 181 (1993) 417.
[9] C. Zaldo, C. Prieto, H. Dexpert, P. Fessler, J. Phys. Condens. Matter. 3 (1991) 4135.
[10] C. Prieto, C. Zaldo, Solid State Commun. 83 (1992) 821.
[11] C. Prieto, C. Zaldo, P. Fessler, H. Dexpert, J.A. Sanz-García, E. Dieguez, F. Agulló-López, Phys. Rev. B 43 (1991) 2594.
[12] C. Mignotte, A. Traverse, P. Moretti, M. Monchanin, Nucl. Instrum. Meth. B 120 (1996) 81.
[13] C. Prieto, Optical Materials 12 (1999) 135.
[14] J. García-Solé, T. Petit, H. Jaffrezic, G. Boulon, Europhys. Lett. 24 (1993) 719.
[15] J. García-Solé, A. Lorenzo, T. Petit, G. Boulon, B. Roux, H. Jaffrecic, J. Phys. IV (France) C4 (1994) 293.
[16] J. García-Solé, Physica Scripta T55 (1994) 30.
[17] A. Lorenzo, H. Jaffrezic, B. Roux, G. Boulon, J. García-Solé, Appl. Phys. Lett. 67 (1995) 3735.
[18] A. Lorenzo, H. Loro, J.E. Muñoz-Santiuste, M.C. Terrile, G. Boulon, L.E. Bausá, J. García-Solé, Opt. Mater. 8 (1997) 55.
[19] D.A. Bryan, R. Gerson, H.E. Tomasche, Appl. Phys. Lett. 44 (1984) 847.
[20] E. Camarillo et al., J. Phys. Condens. Matter. 7 (1995) 9635.
[21] S.C. Abrahams, J.M. Reddy, J.L. Bernstein, J. Phys. Chem. Solids 27 (1996) 1013.
[22] J.J. Rehr, Jpn. J. Appl. Phys. 32 (1993) 8.